

Short-range charge-ordering correlated elastic anomalies in $\text{La}_{2/3}\text{Sr}_{1/3}\text{FeO}_3$

Kong Hui^{a,*}, Zhu Changfei^{b,**}

^a*School of Metallurgy and Resources, Anhui University of Technology, Maanshan, Anhui 243002, PR China*

^b*Laboratory of Advanced Functional Materials and Devices, Department of Materials Science and Engineering, University of Science and Technology of China, Hefei, Anhui 230026, PR China*

Received 29 October 2012; received in revised form 10 December 2012; accepted 11 December 2012

Available online 25 December 2012

Abstract

The longitudinal and transverse ultrasonic velocities in single-phase polycrystalline $\text{La}_{2/3}\text{Sr}_{1/3}\text{FeO}_3$ have been measured by a conventional pulse-echo-overlap technique at a frequency of 10 MHz. Dramatic anomalies in sound velocities for both longitudinal and transverse modes were observed near 214 K. These abnormal ultrasonic features can be fitted by the mean-field theory, which confirms the presence of the Jahn–Teller effect originating from the Fe^{4+} . However, no obvious anomalies in magnetic and electric properties were found in this temperature range. These results give new evidence for the short-range charge ordering state.

© 2013 Published by Elsevier Ltd and Techna Group S.r.l.

Keywords: Transition metal alloys and compounds; Electron–phonon interaction; Ultrasonic

1. Introduction

The perovskite-type transition-metal oxides have attracted much attention due to their interesting structural, magnetic, and electronic properties [1,2]. Among them, $\text{La}_{1-x}\text{Sr}_x\text{FeO}_3$ system is unique because of its special features.

On the one hand, $\text{La}_{1-x}\text{Sr}_x\text{FeO}_3$ system exhibits complex charge ordering (CO) phenomena [3]. At high doping levels ($0.5 \leq x \leq 0.7$), charge ordering transition accompanies both antiferromagnetic (AFM) ordering and charge disproportionation (CD) of $2\text{Fe}^{4+} \rightarrow \text{Fe}^{3+} + \text{Fe}^{5+}$ [4,5]. In this ordering state, iron ions are ordered in the sequence ... $\text{Fe}^{3+} \text{Fe}^{3+} \text{Fe}^{5+} \text{Fe}^{3+} \text{Fe}^{3+} \text{Fe}^{5+}$... along the pseudo-cubic [111] direction. While at low doping levels ($0.3 \leq x \leq 0.4$), a short-range CO state of Fe^{3+} and Fe^{4+} was supposed to explain the superlattice structure at low temperature [3]. According to this supposition, only in some local areas, there are as many Fe^{4+} ions as Fe^{3+} ions

to form the charge ordering state. Thus, this transition cannot be characterized by the measurements of magnetization and resistivity. This hypothesis still needs more evidences.

On the other hand, in $\text{La}_{1-x}\text{Sr}_x\text{FeO}_3$ system, the lattice distortion around CO transition is under discussion. According to the previous studies, it is known that the CO transition in manganites always accompanies the Jahn–Teller distortion of Mn^{3+} [6–8]. Since Fe^{4+} is isoelectronic with Mn^{3+} , the similar lattice distortion is expected in $\text{La}_{1-x}\text{Sr}_x\text{FeO}_3$ system. However, controversial conclusions have been drawn in $\text{La}_{1/3}\text{Sr}_{2/3}\text{FeO}_3$ through different experimental and theoretical tools [3–5,9–11]. First, no structural changes accompany the CO–CD transition. This point was supported by the neutron powder diffraction results [9] and unrestricted Hartree–Fock band-structure calculations [10]. Second, the breathing-type distortion of Fe–O octahedron exists below the charge ordering transition temperature (T_{CO}). This conclusion was drawn through the studies of transmission electron microscopy [3] and optical spectroscopy [4]. Third, the lattice distortion is present above the T_{CO} . This viewpoint was proposed through the temperature-dependent micro-Raman study [5]. Moreover, Blasco et al. suggested that the electronic

*Corresponding author. Tel./fax: +86 0555 2315180.

**Corresponding author. Tel./fax: +86 0551 3602938.

E-mail addresses: konghui@ahut.edu.cn (K. Hui),
cfzhu@ustc.edu.cn (Z. Changfei).

localization in $\text{La}_{1/3}\text{Sr}_{2/3}\text{FeO}_3$ arises from an order–disorder transition between dynamic and static distortions [11]. For $\text{La}_{1-x}\text{Sr}_x\text{FeO}_3$ ($0.3 \leq x \leq 0.4$), superlattice reflections were observed below 250 K by transmission electron microscopy [3]. Based on these results, the model of short-range CO state is proposed.

Recently, ultrasonic technology was applied to $\text{La}_{1-x}\text{Sr}_x\text{FeO}_3$ system to explore its physical nature. As a sensitive tool, ultrasonic responses to lattice distortion and CO transition (including short-range CO transition) in transition metal oxides are based on the solidly theoretical and experimental foundations [6–8]. In fact, anomalies in sound velocity have been observed around T_{CO} in $\text{R}_{1/3}\text{Sr}_{2/3}\text{FeO}_3$ ($\text{R} = \text{La}, \text{Pr}$) [12] and $\text{La}_{1/3}\text{Sr}_{2/3}\text{Fe}_{1-x}\text{Mn}_x\text{O}_3$ [13], which confirms the existence of Jahn–Teller effect of Fe^{4+} . In 2012, the systematically ultrasonic study on $\text{La}_{1-x}\text{Sr}_x\text{FeO}_3$ ($1/3 \leq x \leq 0.45$) has been carried out [14]. However, the transverse ultrasonic results and quantitatively theoretical calculation are still lacked. Thus, in this paper, we presented a study of longitudinal and transverse ultrasonic velocities in $\text{La}_{2/3}\text{Sr}_{1/3}\text{FeO}_3$, and applied the mean-field theory to these results. The aim of this work is to provide new evidence for the short-range charge ordering state.

2. Experimental procedure

The polycrystalline sample of $\text{La}_{2/3}\text{Sr}_{1/3}\text{FeO}_3$ was prepared by the solid-state reaction method. Stoichiometric amounts of high purity La_2O_3 , SrCO_3 and Fe_2O_3 powders were well mixed, ground and calcinated at 1373 K, 1423 K, and 1473 K, respectively, in air for 15 h. The finally obtained powders were pressed into pellets at 300 MPa and then sintered at 1573 K in air for 20 h, and cooled to room temperature at a rate of 1 K min^{-1} .

The crystal structure was characterized using a Japan Rigaku MAX-RD powder X-ray diffractometer with $\text{Cu K}\alpha$ radiation ($\lambda = 1.5418 \text{ \AA}$) at room temperature. Results showed that our sample is of single phase with no detectable secondary phases, and the diffraction peaks can be indexed with the space group $R\bar{3}c$ in the hexagonal setting.

The resistivity was measured by the standard four-probe technique. The zero-field-cooled (ZFC) magnetization was measured in an external magnetic field of 100 Oe by a commercial quantum device (SQUID; Quantum Design MPMSXL). The measurements of longitudinal and transverse ultrasonic velocities were carried out on the Matec-7700 series by means of the conventional pulse-echo-overlap technique.

3. Results and discussion

The temperature dependences of the longitudinal and transverse ultrasonic velocities (V_l and V_t) for $\text{La}_{2/3}\text{Sr}_{1/3}\text{FeO}_3$ are displayed in Fig. 1. It can be seen that both V_l and V_t smoothly soften as the temperature decreases from higher temperature and substantially increases below

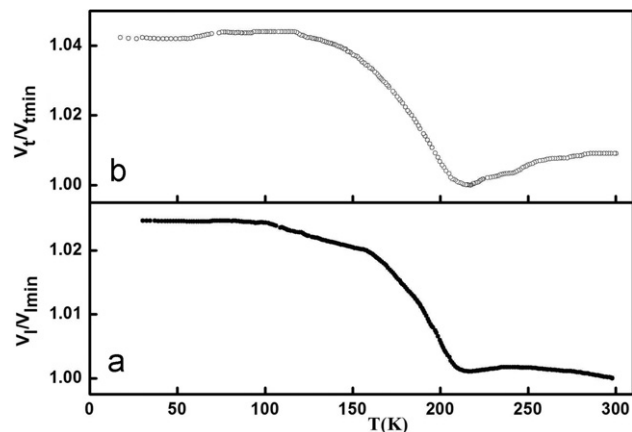


Fig. 1. Temperature dependences of ultrasonic velocities for $\text{La}_{2/3}\text{Sr}_{1/3}\text{FeO}_3$. (a) Longitudinal velocity (V_l). (b) Transverse velocity (V_t).

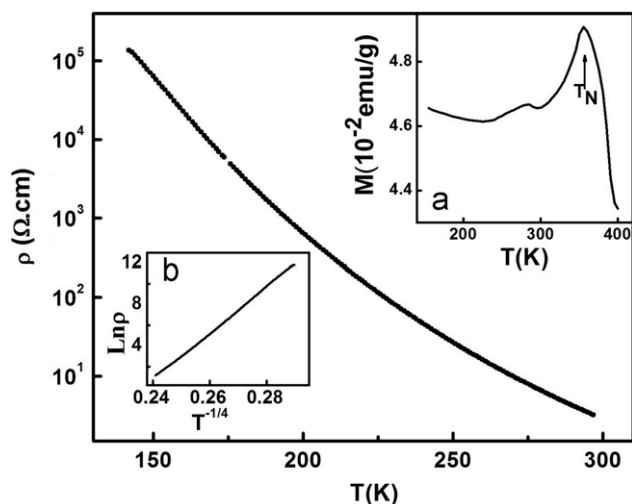


Fig. 2. Temperature dependence of resistivity (ρ) for $\text{La}_{2/3}\text{Sr}_{1/3}\text{FeO}_3$. Inset (a) is the temperature dependence of magnetization. Inset (b) shows $\ln \rho$ vs. $T^{-1/4}$.

214 K, and the relative increase in velocity is more than 2% in both modes. Since the AFM transition temperature is about 350 K (T_N , shown in Fig. 2), it is impossible to correlate these ultrasonic anomalies with magnetic transition.

In fact, the similar ultrasonic feature was observed in $\text{La}_{1/3}\text{Sr}_{2/3}\text{FeO}_3$ around T_{CO} , which is attributed to the Jahn–Teller effect of Fe^{4+} [12]. Since Fe^{4+} also exists in $\text{La}_{2/3}\text{Sr}_{1/3}\text{FeO}_3$, it is reasonable to attribute these ultrasonic anomalies to the similar effect. To better understand the Jahn–Teller effect of Fe^{4+} , the detailed discussions are shown below.

On the one hand, for Fe^{4+} , due to its unconventionally high valency, its charge-transfer energy is quite negative, which means that a large amount of charges are transferred via Fe–O bonds from the O 2p bands to the Fe d orbitals. Thus the Fe^{4+} state is a mixture of high-spin $3d^4$

and $3d^5L$ (L denotes a hole in the O 2p band), and dominated by the $3d^5L$ configuration [15].

On the other hand, for high-spin Fe^{4+} ($3d^4$), one unpaired electron resides in the two-fold degenerate e_g levels. Thus, it is Jahn–Teller active in an octahedral crystal field. According to the Jahn–Teller theory, when this unpaired electron localizes due to charge ordering transition, lattice distortion will be induced to reduce the electrostatic interaction, which leads to the ultrasonic anomaly. For example, in short-range charge ordered manganites $(Nd_{0.75}Na_{0.25})_x(Nd_{0.5}Ca_{0.5})_{1-x}MnO_3$, the Jahn–Teller effect of Mn^{3+} induces a softening of ultrasonic velocity above T_{CO} and a hardening below T_{CO} [8]. This feature was qualitatively similar to our observation. Thus, the ultrasonic anomalies in $La_{2/3}Sr_{1/3}FeO_3$ possibly originate from the Jahn–Teller effect of Fe^{4+} .

Since Fe^{4+} is dominated by the $3d^5L$ configuration, the resulting Jahn–Teller effect of high-spin $3d^4$ is much small, which can reflect on the ultrasonic results. It is known that the relative stiffening of ultrasonic velocity can be viewed as a scale of the development of Jahn–Teller effect [16]. From Fig. 1, it can be seen that the relative increase is about 2.5% for longitudinal ultrasonic velocity. While in representative sample of charge ordered manganites, such as $La_{0.25}Ca_{0.75}Mn_{0.93}Cr_{0.07}O_3$, this value is more than 20%

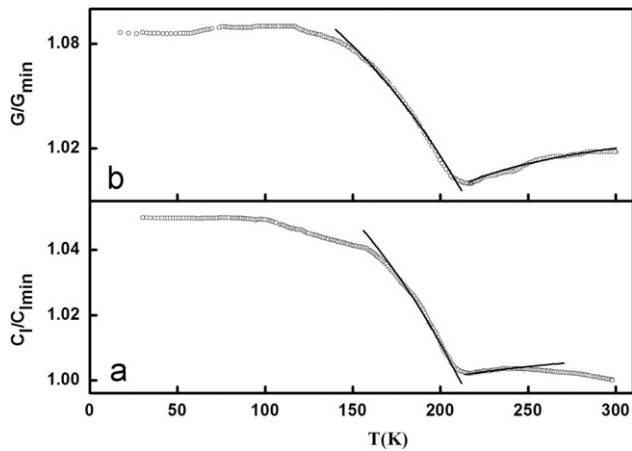


Fig. 3. (a) Temperature dependence of the longitudinal modulus $C_l(T)$. (b) Temperature dependence of the transverse modulus $G(T)$. Open symbols are the experimental data, and solid lines are the results calculated using Eqs. (1) and (2).

[17]. So the resulting lattice distortion in $La_{0.25}Ca_{0.75}Mn_{0.93}Cr_{0.07}O_3$ can be detected by the XRD measurement, while the Jahn–Teller effect of Fe^{4+} is too weak to be detected by neutron diffraction.

To further verify this Jahn–Teller effect, theoretical results were applied to $La_{2/3}Sr_{1/3}FeO_3$. Through the ultrasonic measurements, two kinds of elastic modulus can be calculated. There are longitudinal modulus ($C_l(T) = \rho V_l^2$) and transverse modulus ($G(T) = \rho V_t^2$) [18,19]. In these formulas, ρ is the mass density.

Through Hamiltonian calculation, Melcher gave the relationship between modulus and temperature [20]. These formulas can be used in different temperature ranges.

For the $T > T_{CO}$

$$C(T) = C_0(T - T_C^0)/(T - \Theta) \quad (1)$$

where C_0 is the modulus at absolute zero temperature, and the characteristic temperatures of T_C^0 and Θ can be determined by the ultrasonic measurements of the elastic modulus softening.

For the $T < T_{CO}$

$$\frac{C(T)}{C_0} = \left[1 - \frac{\lambda + \mu}{k_B T} + \frac{\lambda + \mu}{k_B T} \tanh^2\left(\frac{\Delta}{k_B T}\right) \right] / \left[1 - \frac{\lambda}{k_B T} + \frac{\lambda}{k_B T} \tanh^2\left(\frac{\Delta}{k_B T}\right) \right] \quad (2)$$

where λ is the phonon exchange constant, μ is a measure of the strength of the coupling of the ions to the uniform strain, and Δ represents the effect of the ion–strain coupling, which can be written as:

$$\Delta = k_B T_{CO} \tanh\left(\frac{\Delta}{k_B T}\right) \quad (3)$$

In Fig. 3, the open symbols are the experimental data and the solid lines are the theoretical results (the corresponding values of parameters are shown in Table 1). The good agreement between the experimental data and theory indicates that the Jahn–Teller effect indeed exists in $La_{2/3}Sr_{1/3}FeO_3$. This effect is induced by the localization of unpaired electron in e_g levels, which means the occurrence of charge ordering transition.

Normally, charge ordering transition accompanies both AFM ordering and a sharp increase in resistivity [12,13]. However, the T_N of $La_{2/3}Sr_{1/3}FeO_3$ is much higher than

Table 1

Fitting parameters for the longitudinal and transverse modulus, using Eqs. (1) and (2) for $La_{2/3}Sr_{1/3}FeO_3$.

Temperature range	Modulus type	C_0/C_{min}	T_C^0 (K)	Θ (K)
$T > T_{CO}$	Longitudinal	1.015	56.16	54.08
	Transverse	1.047	104.9	99.8
Temperature range	Modulus type	C_0/C_{min}	λ (meV)	μ (meV)
$T < T_{CO}$	Longitudinal	1.08	5.45	1
	Transverse	1.13	5.05	1.63

the temperature of ultrasonic anomalies. And from the inset (b) of Fig. 2, it can be seen that the resistivity can be fitted by Mott's law ($R = R_0 \exp(T_0/T)^{1/4}$), and the expectant anomaly is absent. These unique behaviors are probably due to the nature of short-range charge ordering. According to Li et al.'s hypothesis [3], the short-range charge ordering state of ... $\text{Fe}^{3+}\text{Fe}^{4+}\text{Fe}^{3+}\text{Fe}^{4+}$... only exists in some local areas. Moreover, the results of transmission electron microscopy indicate that this short-range charge ordering transition is gradually developed over a wide temperature range (from 250 K to 150 K). Thus, the measurements of resistivity and magnetization could not respond to this local CO transition. While due to the sensitivity to Jahn–Teller effect, the ultrasonic method can characterize the formation of short-range charge ordering state. The similar phenomenon has also been observed in other short-range charge ordering systems, such as $(\text{Nd}_{0.75}\text{Na}_{0.25})_x(\text{Nd}_{0.5}\text{Ca}_{0.5})_{1-x}\text{MnO}_3$ samples [8].

4. Conclusion

In summary, we have studied the longitudinal and transverse ultrasonic velocities in single-phase polycrystalline $\text{La}_{2/3}\text{Sr}_{1/3}\text{FeO}_3$. Dramatic increases in V_l and V_t are observed below 214 K. These abnormal ultrasonic features can be described by the mean-field theory, which confirms the presence of Jahn–Teller effect originating from the Fe^{4+} . However, no obvious anomalies in magnetic and electric properties were found in this temperature range. The analysis suggests that these results may be explained by the formation of short-range charge ordering state.

Acknowledgment

This work was supported by the National Natural Science Foundation of China (No.11004002).

References

- [1] S. Jin, T.H. Tiefel, R. Ramesh, L.H. Chen, Thousandfold change in resistivity in magnetoresistive La–Ca–Mn–O films, *Science* 264 (1994) 413–415.
- [2] J.Y. Gu, B. Ogale, M. Rajeswari, T. Venkatesan, R. Ramesh, V. Radmilovic, U. Dahmen, G. Thomas, T.W. Noh, In-plane grain boundary effects on the magnetotransport properties of $\text{La}_{0.7}\text{Sr}_{0.3}\text{MnO}_{3-\delta}$, *Applied Physics Letters* 72 (1998) 1113–1115.
- [3] J.Q. Li, Y. Matsui, S.K. Park, Y. Tokura, Charge ordered states in $\text{La}_{1-x}\text{Sr}_x\text{FeO}_3$, *Physical Review Letters* 79 (1997) 297–300.
- [4] S.K. Park, T. Ishikawa, Y. Tokura, J.Q. Li, Y. Matsui, Variation of charge-ordering transitions in $\text{R}_{1/3}\text{Sr}_{2/3}\text{FeO}_3$ ($\text{R}=\text{La}, \text{Pr}, \text{Nd}, \text{Sm}$, and Gd), *Physical Review B* 60 (1999) 10788–10795.
- [5] S. Ghosh, N. Kamaraju, M. Seto, A. Fujimori, Y. Takeda, S. Ishiwata, S. Kawasaki, M. Azuma, M. Takano, A.K. Sood, Raman scattering in CaFeO_3 and $\text{La}_{0.33}\text{Sr}_{0.67}\text{FeO}_3$ across the charge-disproportionation phase transition, *Physical Review B* 71 (2005) 245110–245116.
- [6] B.I. Min, J.D. Lee, S.J. Youn, Lattice dynamics in colossal magnetoresistance manganites, *Journal of Magnetism and Magnetic Materials* 171 (1998) 881–883.
- [7] A.P. Ramirez, P. Schiffer, S.-W. Cheong, C.H. Chen, W. Bao, T.T.M. Palstra, P.L. Gammel, D.J. Bishop, B. Zegarski, Thermodynamic and electron diffraction signatures of charge and spin ordering in $\text{La}_{1-x}\text{Ca}_x\text{MnO}_3$, *Physical Review Letters* 76 (1996) 3188–3191.
- [8] L. Jiang, J.R. Su, H. Kong, Y. Liu, S.Y. Zheng, C.F. Zhu, Ultrasonic study of the charge mismatch effect in charge-ordered $(\text{Nd}_{0.75}\text{Na}_{0.25})_x(\text{Nd}_{0.5}\text{Ca}_{0.5})_{1-x}\text{MnO}_3$, *Journal of Physics: Condensed Matter* 18 (2006) 8563–8571.
- [9] P.D. Battle, T.C. Gibb, P. Lightfoot, The structural consequences of charge disproportionation in mixed-valence iron oxides. I. The crystal structure of $\text{Sr}_2\text{LaFe}_3\text{O}_{8.94}$ at room temperature and 50 K, *Journal of Solid State Chemistry* 84 (1990) 271–279.
- [10] J. Matsuno, T. Mizokawa, A. Fujimori, K. Mamiya, Y. Takeda, S. Kawasaki, M. Takano, Photoemission and Hartree–Fock studies of oxygen-hole ordering in charge-disproportionated $\text{La}_{1-x}\text{Sr}_x\text{FeO}_3$, *Physical Review B* 60 (1999) 4605–4608.
- [11] J. Blasco, B. Aznar, J. Garcia, G. Subias, J. Herrero-Martín, J. Stankiewicz, Charge disproportionation in $\text{La}_{1-x}\text{Sr}_x\text{FeO}_3$ probed by diffraction and spectroscopic experiments, *Physical Review B* 77 (2008) 054107–054116.
- [12] H. Kong, C.F. Zhu, Variation of ultrasonic behaviors in $\text{R}_{1/3}\text{Sr}_{2/3}\text{FeO}_3$ ($\text{R}=\text{La}, \text{Pr}, \text{Gd}$), *Europhysics Letters* 86 (2009) 54001–54005.
- [13] H. Kong, C.F. Zhu, The Mn-doping effect on the charge ordering state of $\text{La}_{1/3}\text{Sr}_{2/3}\text{FeO}_3$, *Journal of Alloys and Compounds* 509 (2011) 731–734.
- [14] H. Kong, S. Shao, C.F. Zhu, Ultrasonic evidence for short-range charge-ordering state in the low-doping regime of $\text{La}_{1-x}\text{Sr}_x\text{FeO}_3$ ($1/3 \leq x \leq 0.45$), *Phase Transitions* 85 (2012) 840–846.
- [15] M. Abbate, F.M.F. de Groot, J.C. Fuggle, A. Fujimori, O. Strelbel, F. Lopez, M. Domke, G. Kaindl, G.A. Sawatzky, M. Takano, Y. Takeda, H. Eisaki, S. Uchida, Controlled-valence properties of $\text{La}_{1-x}\text{Sr}_x\text{FeO}_3$ and $\text{La}_{1-x}\text{Sr}_x\text{MnO}_3$ studied by soft-X-ray absorption spectroscopy, *Physical Review B* 46 (1992) 4511–4519.
- [16] R.K. Zheng, G. Li, Y. Yang, A.N. Tang, W. Wang, T. Qian, X.G. Li, Transport, ultrasound, and structural properties for the charge-ordered $\text{Pr}_{1-x}\text{Ca}_x\text{MnO}_3$ ($0.5 \leq x \leq 0.875$) manganites, *Physical Review B* 70 (2004) 014408–014414.
- [17] X.-G. Li, H. Chen, C.F. Zhu, H.D. Zhou, R.K. Zheng, J.H. Zhang, L. Chen, Ultrasonic study on charge ordering, magnetic, and structural changes in $\text{La}_{0.25}\text{Ca}_{0.75}\text{Mn}_{0.93}\text{Cr}_{0.07}\text{O}_3$, *Applied Physics Letters* 76 (2000) 1173–1175.
- [18] M. Cankurtaran, G.A. Saunders, K.C. Goretta, R.B. Poeppel, Ultrasonic determination of the elastic properties and their pressure and temperature dependences in very dense $\text{YBa}_2\text{Cu}_3\text{O}_{7-x}$, *Physical Review B* 46 (1992) 1157–1165.
- [19] V. Rajendran, S.K. Muthu, V. Sivaubramanian, T. Jayakumar, Raj. Baldev, Anomalies in elastic moduli and ultrasonic attenuation near ferromagnetic transition temperature in $\text{La}_{0.67}\text{Sr}_{0.33}\text{MnO}_3$ perovskite, *Physica Status Solidi A* 195 (2003) 350–358.
- [20] R.L. Melcher, The anomalous elastic properties of materials undergoing cooperative Jahn–Teller phase transitions, in: W.P. Maston, R.N. Thurston (Eds.), *Physical Acoustics*, Academic Press, New York, 1970, pp. 1–21.